Bioinspiration & Biomimetics

NOTE

Effects of flight altitude on the lift generation of monarch butterflies: from sea level to overwintering mountain

Madhu K Sridhar[1], Chang-Kwon Kang[1,*], D Brian Landrum[1], Hikaru Aono[2], Shannon L Mathis[3] and Taeyoung Lee[4]

[1] Department of Mechanical and Aerospace Engineering, University of Alabama in Huntsville, AL 35899, United States of America
[2] Department of Mechanical Engineering and Robotics, Shinshu University, Ueda, Nagano, 386-8567, Japan
[3] Department of Kinesiology, University of Alabama in Huntsville, AL 35899, United States of America
[4] Department of Mechanical and Aerospace Engineering, George Washington University, Washington, DC 20052, United States of America
[*] Author to whom any correspondence should be addressed.

E-mail: chang-kwon.kang@uah.edu

Keywords: monarch butterflies, high-altitude flight, lift coefficient

Supplementary material for this article is available online

RECEIVED
20 August 2020

REVISED
12 November 2020

ACCEPTED FOR PUBLICATION
28 January 2021

PUBLISHED
19 March 2021

Abstract

Aerodynamic efficiency behind the annual migration of monarch butterflies, the longest among insects, is an unsolved mystery. Monarchs migrate 4000 km at high-altitudes to their overwintering mountains in Central Mexico. The air is thinner at higher altitudes, yielding reduced aerodynamic drag and enhanced range. However, the lift is also expected to reduce in lower density conditions. To investigate the ability of monarchs to produce sufficient lift to fly in thinner air, we measured the climbing motion of freely flying monarchs in high-altitude conditions. An optical method was used to track the flapping wing and body motions inside a large pressure chamber. The air density inside the chamber was reduced to recreate the higher altitude densities. The lift coefficient generated by monarchs increased from 1.7 at the sea-level to 9.4 at 3000 m. The correlation between this increase and the flapping amplitude and frequency was insignificant. However, it strongly correlated to the effective angle of attack, which measures the wing to body velocity ratio. These results support the hypothesis that monarchs produce sufficiently high lift coefficients at high altitudes despite a lower dynamic pressure.

1. Introduction

Insects including butterflies rely on flapping motions to generate lift which is enhanced due to several unsteady mechanisms [1–4]. Butterflies have a large pair of flexible wings relative to their body [5] which flap at a relatively low frequency compared to fruit flies and bumblebees. Their low flapping frequency dynamics are closely coupled to instantaneous aerodynamics [6–11].

An amazing feat accomplished by the monarchs is their annual migration. Monarch butterflies fly from eastern North America to high mountains of Central Mexico in the fall [12], the longest migration among insects [13, 14]. During the course of three months [13, 15, 16], hundreds of millions of monarchs migrate a distance of 4000 km, which translates to about 80 million times their average body length. In comparison, 80 million times the average human height yields a distance of 140 000 km, which is about 3.5 times the circumference of the Earth. This normalized range exhibited by the monarchs is orders of magnitudes longer than those of man-made aircraft. For example, the longest passenger aircraft route is 15 344 km from New York to Singapore, which is approximately 229 000 Airbus A350 body lengths.

Unable to obtain significant nectar during the winter, monarchs depend on their stored lipid reserves for at least three months during their overwintering period [15]. Furthermore, the high-altitude forest ecosystem of their overwintering sites is believed to lower their metabolic rates [13, 15]. A study of the monarch genomes found that the strongest signatures of selection associated with migration center on flight muscle function, resulting in a greater flight efficiency [17]. These findings

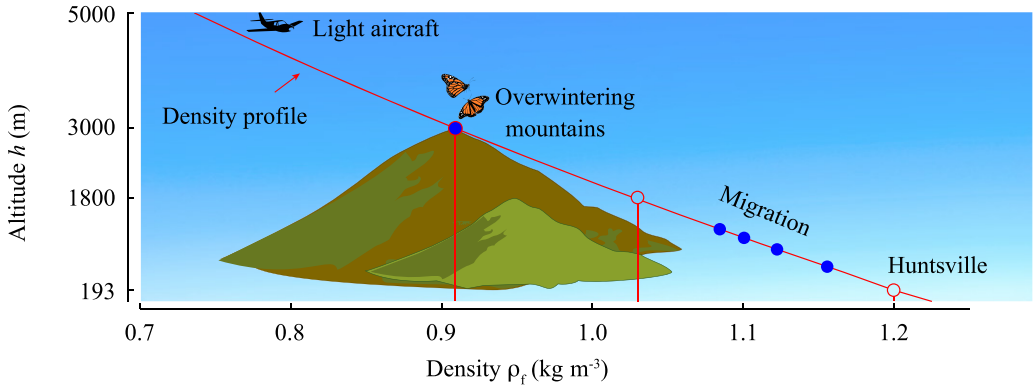

Figure 1. Altitudes achieved by monarch butterflies during migration and the corresponding density profile. Red open circles denote altitudes considered in the current study and blue dots indicate the reported monarch sighting altitudes [14]. Reproduced from [58–60]. CC BY 4.0.

suggest that their motion at these high-altitudes is highly efficient. However, the aerodynamic mechanism behind the long-range migration is inadequately understood.

Glider pilots have spotted migrating monarchs as high as 1250 m [14, 18]. All of their overwintering sites in Mexico are located at altitudes between 2900 m and 3300 m [19–21]. Monarchs migrating at high-altitudes [14, 18] can benefit from Earth's boundary layer [22]. Furthermore, at an altitude of 3000 m, the air density is only 76% of the density at the sea level (figure 1). The aerodynamic drag, which is proportional to the air density, decreases with altitude. A minimal aerodynamic drag is critical to enable the long-range migration. An intriguing part of this problem is that the lift, required to stay aloft during the long-range migration, is also expected to decrease proportionately to the lower density at higher altitudes. Butterflies rely on intermittent flapping and gliding [23, 24] to generate propulsive forces, which are inherently coupled to the drag. On the other hand, man-made aircraft and helicopters use engines to produce thrust, a fundamentally different mechanism and independent from aerodynamic force generation on the wings. This study is driven by the hypothesis that the monarch butterflies generate higher lift coefficients at higher altitudes to compensate for the lower density.

Most insect motion measurements that consider tethered flight [25] or hover flight [26] do not represent the actual motion in free flight [27, 28]. The main difficulty in the conventional method [29, 30] to record kinematic data of a freely flying insect is that it must fly through a relatively small volume that is in full camera view, not suitable for measuring freely flying monarchs. Monarchs are relatively slowly flapping (10 Hz), large (5 cm wing length) butterflies, requiring a large capture volume to record the motion. Furthermore, the literature lacks data on freely flying monarchs in high altitude conditions as the high altitude conditions are not easily reproduced.

To study the effects of a high-altitude environment on the lift, we measured the free flight of monarchs in a large pressure chamber. The air density inside the chamber was reduced to simulate high-altitude conditions between 193 m (Huntsville, AL) and 3000 m (characteristic of overwintering sites in Mexico). In this study we focused on flapping climbing trajectories. Climbing is an energetically costly mode of locomotion [31]. We aimed to observe and investigate the ability of monarch butterflies to produce lift to climb against gravity. An optical method was used to observe the wing and body motion and the data was used to calculate the resultant flapping angle and forces acting on the butterfly [32]. The wing and body pitch angles as well as passive deformations that can play an important role in the monarch flight were not measured in this study. Rather, we aimed to measure the lift, the resultant force component normal to the trajectory, directly calculated from the measured trajectory and equations of motion without relying on an aerodynamics model. A statistical method was used to test the significance of the flapping angle, effective angle of attack due to the body undulation, and lift coefficient with the altitude.

2. Materials and methods

2.1. High-altitude pressure chamber

The free flight measurements of monarch butterflies were conducted in the University of Alabama in Huntsville Propulsion Research Center pressure chamber (figures 2(a) and S1 in online supplementary material (https://stacks.iop.org/BB/16/034002/mmedia)). The chamber is capable of achieving high vacuum and can maintain a base pressure of 10^{-10} atm.

We considered the density conditions corresponding to the altitude of the experimental facility in Huntsville, AL ($h = 193$ m above sea level), an intermediate altitude ($h = 1800$ m) to simulate the effects of the altitude on the flight of monarch

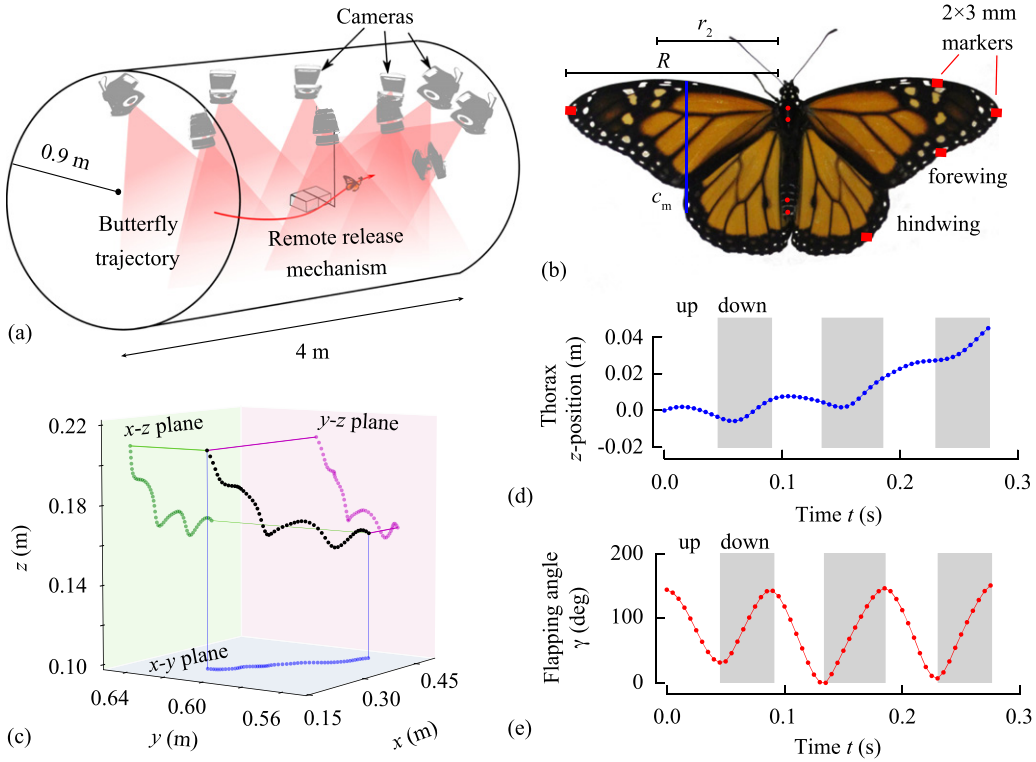

Figure 2. Experimental setup, body and wing kinematics. (a) The butterflies are remotely released in the pressure chamber with motion tracking cameras. (b) Reflective markers are placed on the monarch butterfly wings and body to record their positions. (c) Body position and its projection on the orthogonal planes, (d) thorax vertical position, and (e) flapping angle γ of an example trajectory at an altitude of 3000 m.

butterflies, and the altitude ($h = 3000$ m) for the overwintering mountains in Central Mexico. The density ρ_f decreases from 1.2 kg m^{-3} at $h = 193$ m to 1.03 kg m^{-3} and 0.91 kg m^{-3} at $h = 1800$ m and $h = 3000$ m, respectively [33]. We first recorded the temperature inside the chamber for each altitude. Based on the temperature and the desired air density at the considered altitude per standard atmospheric table [33], we calculated the required chamber pressure using the ideal gas law. We used a pump to control the pressure inside the chamber.

2.2. Butterfly morphology

Monarch butterflies were released remotely inside the pressure chamber. The monarch butterflies (*Dannaus plexippus*) were purchased from Swallowtail farms. The butterfly handling procedures and optical motion tracking procedures are described in our previous study [32]. Four monarch butterfly specimens were used in this study (table 1). Our observation of freely flying monarchs suggests that the monarchs fly with their wings in the overlapped configuration. Therefore, we chose the wing area of all four wings in the overlapped configuration (figure 2(b)) as the wing area S, which was $S = 29 \times 10^{-4}$ m^2 on average. The average length of the right forewing was $R = 53 \times 10^{-3}$ m, defined as the distance between the wing root and the wing tip. The mean chord was $c_m = S/(2R) = 27 \times 10^{-3}$ m. The average non-dimensional radius to the second moment of wing area for the right forewing was $\hat{r}_2 = 0.53$, an important flapping wing aerodynamics metric [34]. The average butterfly weight with markers was $W = 5.5$ mN. The average aspect ratio of the forewing and wing loading were $AR = (2R)^2/S = 4$ and $W/S = 2$ N m^{-2}, respectively.

2.3. Optical marker placement and measurements

We attached reflective rectangular markers of 2×3 mm size, weighing 1.5 mg, to the wings on both the dorsal and ventral sides to capture wing motion in both up and down strokes (figure 2(b)). Two circular markers with a diameter of 1.8 mm and weight of 0.29 mg each were placed on the thorax and two more circular markers of the same size and weight were placed on the abdomen of the butterfly using very small amounts of cyanoacrylate. Ten VICON T40s cameras were installed inside the pressure chamber (figure 2(a)) to track the reflective marker positions and capture the three-dimensional body trajectory and wing kinematics inside the chamber at a sampling rate of 200 Hz for 15 s (figures 2(c)–(e)).

We recorded 81 trajectories from 19 butterfly specimens. We only considered flight measurements that were at least three consecutive flapping cycles long (figure S2 in online supplementary material). The climb angle θ (figure 3) was calculated based on end points of the trajectory. In order to compare kinematics for similar trajectories and, hence,

Table 1. Morphological parameters for four monarch butterfly specimens. The fore and hindwing areas are denoted by S_{FW} and S_{HW}, respectively.

		Wing area ($\times 10^{-4}$m^2)						
W (mN)	R ($\times 10^{-3}$m)	S_{FW}	S_{HW}	S	c_m ($\times 10^{-3}$ m)	W/S (N m^{-2})	AR	$\hat{r}_2$
5.3	52	22	18	32	31	1.7	3.4	0.54
5.8	54	21	14	34	32	1.7	3.4	0.54
5.7	52	17	13	26	25	2.2	4.1	0.54
5.2	52	15	12	22	21	2.3	4.9	0.51

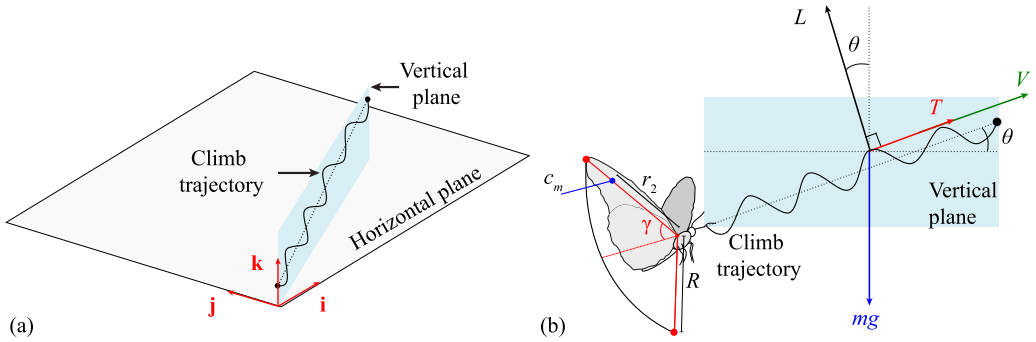

Figure 3. A schematic showing the definition of the lift and thrust. (a) We first determine the vertical plane containing the end points of the thorax trajectory where **i**, **j**, **k** are the unit vectors of the reference frame. (b) The lift L and thrust T are determined by considering the dynamic equilibrium of the butterfly with a climb angle θ on the vertical plane.

similar lift magnitudes, we chose trajectories with climb angle between 11 to 15 deg. Among these, we considered those trajectories which exhibit minimum turning. The roll motion along the longitudinal axis of the body can be assumed to be minimal for straight trajectories without significant lateral turning. Thus, the left and the right wing motions can be assumed to be symmetric about the longitudinal plane. There were four trajectories of the four butterfly specimens (table 1) that met these conditions.

The positions of missing marker data points were estimated using a cubic spline interpolation method. Among the four trajectories considered, the range of interpolation required for the markers varied between 2% and 38% of the three flapping cycles. The difference in the mean flapping angle in three flapping cycles due to the uncertainty of thorax marker choice was 0.44%. The data were filtered using a Butterworth fourth order filter with a cutoff frequency of 35 Hz to remove high frequency noise.

2.4. Calculation of wing kinematics and body motion

Figure 2(c) shows the three-dimensional trajectory recorded inside the pressure chamber at density altitude of 3000 m with a climb angle of 12 deg. We calculated the thorax velocity from the position of the thorax marker. The thorax velocity $\boldsymbol{V}$ for a single flapping cycle was determined by considering the end points of the thorax trajectory of the flapping cycle. Note that the environmental differences between controlled and natural conditions can have certain influences on flight speed of butterflies [35]. We applied the second order central difference scheme twice on the instantaneous interpolated and filtered position of thorax marker to determine its instantaneous acceleration. All observed trajectories of the thorax followed an undulating path (figure 2(d)).

The left and right forewing tip markers in combination with the thorax marker were used to calculate the angle between the left and the right forewings (figure S3 in online supplementary material). The flapping angle γ was defined as half of the angle between the left and right forewings. The flapping frequency f was determined using a fast Fourier transform of the flapping angle time history. The flapping amplitude was calculated as $\gamma_a = (\gamma_{max} - \gamma_{min})/2$, where γ_{min} and γ_{max} are the flapping angles at the beginning and end of the downstroke, respectively. The flapping angle γ (figure 2(e)) was nearly sinusoidal with a peak at the end of the downstroke. The flapping angle was approximated as a first order harmonic $\gamma_{FH}(t) = \gamma_a \cos(2\pi ft)$ in our analysis.

2.5. Calculation of lift and thrust forces in climbing trajectory

The acceleration of the thorax $\boldsymbol{A}$ was multiplied by the butterfly mass m and added to the weight to obtain the resultant force acting on the butterfly as $\boldsymbol{F} = m\boldsymbol{A} + mg\mathbf{k}$ (figure 3), where g is the gravitational acceleration. To calculate lift and thrust, we first determined the vertical plane that includes **k** and the straight line (figure 3(a)) joining the trajectory end points for each motion cycle. The lift L is the component of $\boldsymbol{F}$ normal to this line in the

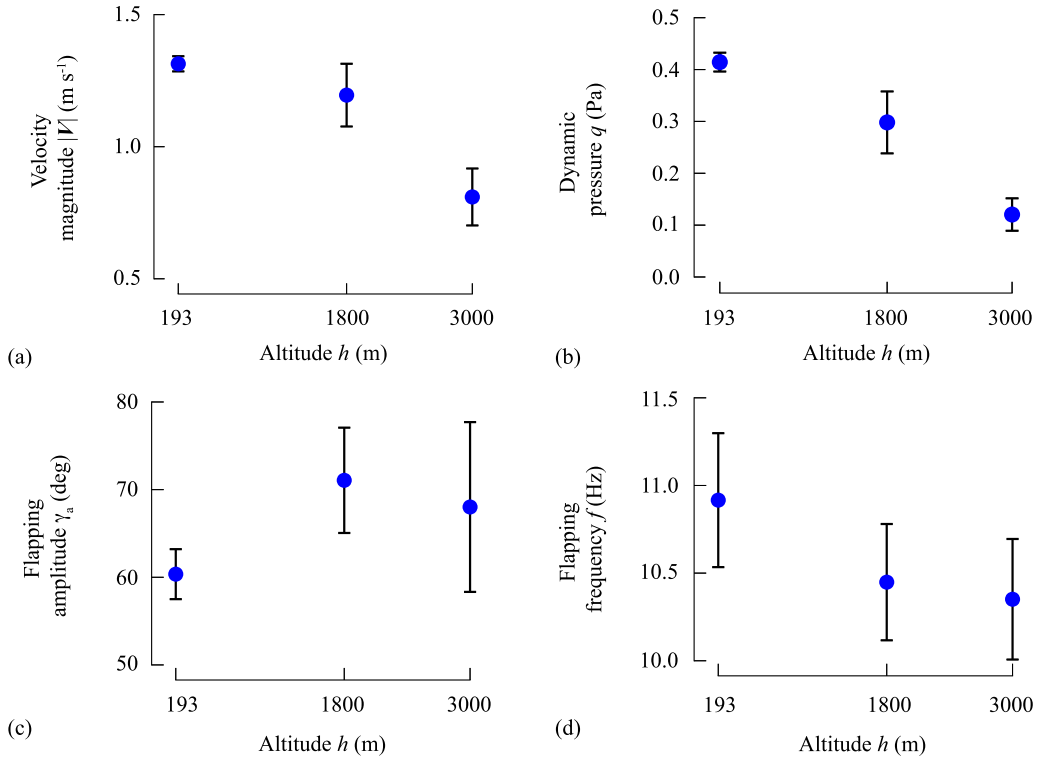

Figure 4. Variation of body and wing motions with altitude. Mean and 95% confidence intervals (standard error) for the (a) thorax velocity magnitude $|\boldsymbol{V}|$, (b) dynamic pressure q, (c) flapping amplitude γ_a, and (d) flapping frequency f are shown at each altitude h. The sample size n which corresponds to the number of individual cycles is $n = 3$ at $h = 193$ m and $h = 3000$ m and $n = 6$ at $h = 1800$ m.

vertical plane and the thrust T is the component tangential to this line (figure 3(b)). This direct method avoids influences from modeling uncertainties associated with the existing flapping wing aerodynamics models including the Navier–Stokes equation models. These models calculate the lift and drag based on the wing motion. However, the effects of wing flexibility or coupling to body dynamics on the calculation of lift are very difficult to model.

We computed cycle-averaged quantities, denoted by $\langle\bullet\rangle$, separately for each individual flapping cycle from the time histories (figure S4 in online supplementary material). The mean quantities, denoted by $\bar{\bullet}$, are arithmetic means of a cycle-averaged quantity over the number of flapping cycles at the considered altitude.

2.6. Statistical data analysis

We used four butterfly specimens in the current study: one specimen each at 193 m and 3000 m, and two specimens at 1800 m. A linear mixed-effect model with a butterfly as a random effect was used to determine differences in dependent variables across three altitudes. The mixed-model with butterfly as a random effect allows for repeated measures within butterfly. An individual butterfly was chosen as the random effect because the dataset consisted of clusters of repeated measurements using an individual butterfly specimen. Data were analyzed using Stata statistical analysis software (Version 14.0; StataCorp, College Station, TX, USA). Statistical significance was set at 0.05 for all analyses (two-tailed).

3. Results and discussion

3.1. Effects of wing/body kinematics

Using a linear mixed-effect model with the butterfly as a random effect (section 2.6), an increase in altitude between 193 m and 3000 m resulted in a decrease in the mean thorax speed $|\overline{\boldsymbol{V}}|$ (figure 4(a)) from 1.3 m s^{-1} to 0.8 m s^{-1} ($z = -2.87$, $p = 0.004$, 95% CI $= [-0.000\,29, -0.000\,05]$). The resulting dynamic pressure $q = 0.5\rho_f|\boldsymbol{V}|^2$ (figure 4(b)) also decreased with altitude. The mean flapping amplitude of the right forewing remained within an interval of $\overline{\gamma}_a = 60$ deg and $\overline{\gamma}_a = 68$ deg ($z = 1.26$, $p = 0.209$, 95% CI $= [-0.001\,71, 0.007\,83]$) between 193 m and 3000 m (figure 4(c)). The change with altitude was not statistically significant. The mean flapping frequency showed a minor variation between 10.9 Hz and 10.4 Hz ($z = -2.20$, $p = 0.028$, 95% CI $= [-0.000\,40, -0.000\,02]$), indicating that the altitude effects on flapping frequency was minimal (figure 4(d)).

The first natural frequency of the wing f_1, which is a structural parameter related to the monarch wings, only depends on the wing structure and is unaffected by the surrounding fluid density. Hence the frequency ratio f/f_1 [36] remains unaffected by the change in

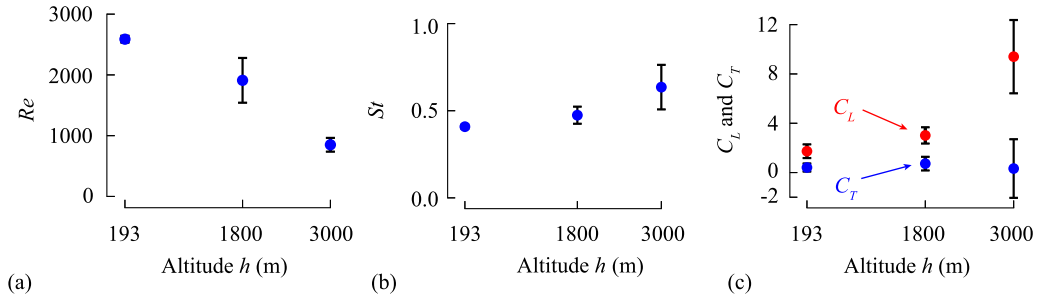

Figure 5. Variation of non-dimensional parameters with altitude. Mean and 95% confidence intervals (standard error) for the (a) Reynolds number *Re*, (b) Strouhal number *St* (c) lift coefficient C_L and thrust coefficient C_T. Statistical results are provided in table 2.

air density with altitude. In addition to this inertial effect, the structural dynamics response of the highly flexible monarch wing is influenced by the aerodynamic forces including the added mass. For example, the non-dimensional relative wing deformation $\delta = 2(1+\pi/(4\rho^* h_s^*))/(k((f_1/f)^2-1))$, where $\rho^* = \rho_s/\rho_f$ and $h_s^* = h_s/c_m$, measures the interplay between the inertial, added mass, and structural dynamic balance [37, 38]. This scaling parameter depends on the air density ρ_f and we expect the wing motion and the aerodynamic performance to be affected by the air density.

That said, all observations of the monarch flight characteristics reported in this study includes any effects of the fluid–structure interaction. For example, the flapping angle γ (section 2.4) includes the outcome of the effects of the wing deformation due to wing flexibility. Furthermore, the resulting lift and thrust were calculated based on the dynamics of the monarch flight, including the effects of wing flexibility as discussed in section 2.5.

3.2. Aerodynamics coefficients, Reynolds number and effective angle of attack

We used the flight velocity measured at the body as the reference velocity scale consistently throughout the study in the definition of relevant non-dimensional parameters. This choice is consistent with other studies of flying animals in forward flight [39–44]. Moreover, the body velocity can be used to characterize the gliding flight of the monarchs, whereas a wing velocity scale cannot be used. In flapping wing aerodynamics studies that consider hovering flight, the wing velocity is used as the reference velocity. In these studies, the main aerodynamic force of interest, e.g. lift in hover, averaged over a flapping cycle is perpendicular to the wing motion. On the other hand, we focused on the monarch lift generation, where the lift is perpendicular to the body velocity (figure 3(b)) [45], a situation similar to that of aircraft aerodynamics. This lift is parallel to the wing motion.

The Reynolds number (figure 5(a)), a key non-dimensional variable, is calculated based on mean chord c_m and body velocity as $Re = \rho_f |\boldsymbol{V}| c_m/\mu$, where μ is the dynamic viscosity. The Reynolds number decreased from $\bar{Re} = 2588$ at $h = 193$ m to $\bar{Re} = 850$ at $h = 3000$ m ($z = -3.65, p < 0.001$, 95% CI $= [-0.926\,09, -0.279\,54]$).

Table 2. Mean kinematic and aerodynamic quantities for the three altitudes.

	Altitude h (m)				
	193	1800	3000	z	p-value
$\overline{\gamma}_a$ (deg)	60	71	68	1.26	0.209
$\overline{f}$ (Hz)	10.9	10.4	10.3	-2.20	0.028
$\overline{\lvert \boldsymbol{V} \rvert}$ (m s^{-1})	1.3	1.2	0.8	-2.87	0.004
$\overline{C}_L$	1.7	3.0	9.4	3.30	0.001
$\overline{C}_T$	0.4	0.7	0.3	-0.05	0.957
$\overline{\alpha}_{\text{eff}}$ (deg)	35	37	43	2.89	0.004
$\bar{Re}$	2588	1911	850	-3.65	< 0.001
$\bar{St}$	0.41	0.47	0.64	3.17	0.002

The ratio between the mean wing speed at r_2 and the body velocity is measured by the Strouhal number $St = 2fr_2 \sin(\gamma_a)/|\boldsymbol{V}|$ [46, 47] (figure 5(b)). Strouhal number increases from $\bar{St} = 0.41$ at $h = 193$ m to $\bar{St} = 0.64$ at $h = 3000$ m ($z = 3.17$, $p = 0.002$, 95% CI $= [0.0003, 0.000\,13]$).

The lift coefficient C_L and the thrust coefficient C_T were obtained by normalizing the lift L and thrust T by $0.5\rho_f |\boldsymbol{V}|^2 S$ [45]. The mean lift did not show significant variation with altitude. This by construction was due to the consideration of trajectories with a narrow range of climb angles. However, the mean lift coefficient $\overline{C}_L$ increased with altitude (figure 5(c) and table 2) from 1.7 to 9.4 ($z = 3.30$, $p = 0.001$, 95% CI $= [0.001\,07, 0.004\,18]$). Conversely, $\overline{C}_T$ decreased slightly, but not statistically significantly, from $\overline{C}_T = 0.4$ to $\overline{C}_T = 0.3$ ($z = -0.05$, $p = 0.957$, 95% CI $= [-0.000\,58, 0.000\,55]$).

3.3. Higher lift coefficients in thinner air

Our free flight measurements show that the mean lift coefficient produced by the monarch butterflies at sea level is 1.7 (figure 5(c)). This lift coefficient magnitude is within the range of what has been observed for other butterflies. For neotropical butterflies in free flight [35], lift coefficients, calculated based on the forward velocity and an air density of 1.23 kg m^{-3},

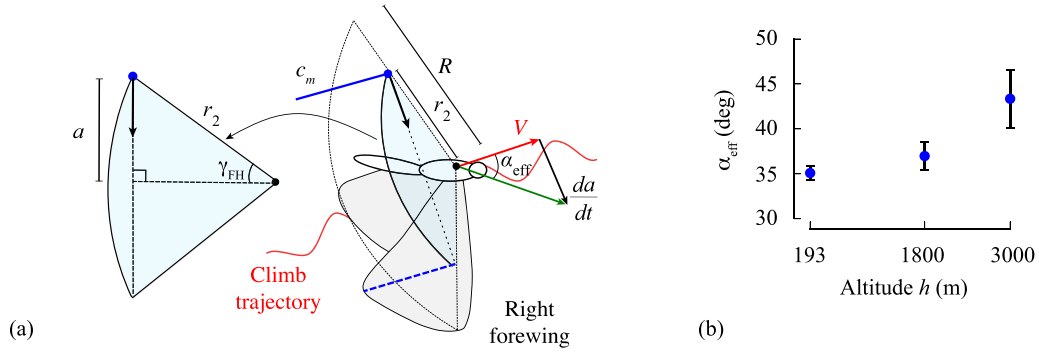

Figure 6. (a) Schematic illustrating the definition of effective angle of attack. The flapping motion of the wing tilts the body effective velocity by α_{eff}. The blue line represents the wing chord and blue dot indicates the position of the leading edge of the right forewing at $r_2 = R\hat{r}_2$ at the beginning of the downstroke. (b) Mean and 95% confidence intervals for the effective angle of attack α_{eff} at each altitude h.

varied between 0.05 and 2.9. Other insects in forward flight, such as fruit flies, generate lift coefficients around 4 [48], bumblebees around 1.3 [49, 50], hawkmoths around 1.7 [51], and dragonflies around 1 [52]. Passenger aircraft typically produce lift coefficients between 1 and 3 [53].

As the air density decreases with the altitude, the observed mean lift coefficient in monarchs increased to 9.4 with a maximum of 12.3 at the overwintering altitude of 3000 m (figure 5(c)). The statistically significant increase in the lift coefficient implies an aerodynamic performance enhancement, suggesting the existence of the beneficial effects of reduced atmospheric density during high-altitude migration. In general, one way to maintain the same level of lift in a lower density environment is to augment the dynamic pressure by flying faster. For example, the kinematics measured for hovering bumblebees in a rarefied environment between 3250 m and 8120 m [54] showed that the bees' flapping amplitude increased with the altitude without changing the flapping frequency, increasing the dynamic pressure [54]. However, the changes in the flapping amplitude and frequency of the monarchs with the altitude (figures 4(c) and (d)) were statically insignificant. Furthermore, the flight speed reduced, resulting in a lower dynamic pressure. The second method is the enhancement of lift coefficient. This increase in the lift coefficient correlated to the increase of the Strouhal number (figure 5(b)).

The effect of the Strouhal number on the lift coefficient can be explained by considering the effective angle of attack. We calculated the wing effective angle of attack α_{eff} as the angle between instantaneous flapping velocity of the wing and the thorax velocity $\boldsymbol{V}$ for each flapping cycle (figure 6(a)) as

$$\alpha_{\text{eff}} = \arctan\left(\frac{\dot{a}}{|\boldsymbol{V}|}\right) = \arctan\left(-\frac{2\pi f r_2 \gamma_a \sin(2\pi f t)\cos(\gamma_{\text{FH}})}{|\boldsymbol{V}|}\right), \quad (1)$$

where $\dot{a} = \mathrm{d}a/\mathrm{d}t$ is the projection of the flapping velocity at the radius of the second moment of wing area $r_2 = R\hat{r}_2$ (figure 6(a)). When $|\dot{a}| \ll |\boldsymbol{V}|$ we can show that $St = \bar{\alpha}_{\text{eff}}/2$ (online supplementary material). For the monarchs $\dot{a}/|\boldsymbol{V}| = \mathcal{O}(1)$. Nevertheless, the trends of St (figure 5(b)) and α_{eff} (figure 6(b)) are similar. Due to the decreasing flight speed relative to the wing velocity, the mean effective angle of attack (figure 6(b)) increased from $\overline{\alpha}_{\text{eff}} = 35$ deg at $h = 193$ m to $\overline{\alpha}_{\text{eff}} = 43$ deg at $h = 3000$ m ($z = 2.89$, $p = 0.004$, 95% CI $= [0.000\,90, 0.004\,72]$). The coefficient of determination of the correlation between the cycle-averaged lift coefficient and cycle-averaged effective angle of attack was 0.936 (figure 7(a)).

A linear regression for $\langle C_L \rangle$ as a function of $\langle \alpha_{\text{eff}} \rangle$ suggests that $\langle C_L \rangle = 49.8\langle \alpha_{\text{eff}} \rangle - 28.8$. The resulting lift curve slope $\mathrm{d}\langle C_L \rangle/\mathrm{d}\langle \alpha_{\text{eff}} \rangle = 49.8$ rad^{-1} is significantly higher compared to the thin airfoil theory predicted slope of 2π rad^{-1} [55]. With $\langle L \rangle = 0.5\rho_{\text{f}}|\boldsymbol{V}|^2 S\langle C_L \rangle$, above linear regression and $\alpha_{\text{eff}} = \arctan(\dot{a}/|\boldsymbol{V}|)$, we can express $\langle L \rangle$ as a function of $|\boldsymbol{V}|$ as $\langle L \rangle = 0.5\rho_{\text{f}}|\boldsymbol{V}|^2 S(49.8 \arctan(\dot{a}/|\boldsymbol{V}|) - 28.8)$. There are two trends indicated by the maximum lift flight speed $V_{L\,\max}$ and the zero lift flight speed $V_{L=0}$ (figure 7(b)). When $|\boldsymbol{V}| < V_{L\,\max}$, lift increases when the monarch flies faster. When $V_{L\,\max} < |\boldsymbol{V}| < V_{L=0}$, lift reduces as $|\boldsymbol{V}|$ increases. The flapping wing motion did not change significantly with the altitude. The mean wing speed remained near $\dot{a} = 1$ m s^{-1}, such that $V_{L\,\max} = 0.92$ m s^{-1} and $V_{L=0} = 1.53$ m s^{-1}. As the air density decreased, the flight speed decreased from 1.3 m s^{-1} at 193 m to 1.2 m s^{-1} at 1800 m and, finally, 0.8 m s^{-1} at 3000 m. This analysis shows that the lift at a given density and wing area indeed increases by flying slower for the observed dynamics. The increase in lift through the effective angle of attack and lift coefficient by lowering $|\boldsymbol{V}|$ outweighs the reduction through $|\boldsymbol{V}|^2$.

The effective angle of attack can also be increased by flapping faster (equation (1)). However, the power consumption scales with $P \sim L\dot{a}$ [56, 57]. Maintaining the same level of lift in thinner air by flapping faster (increasing $\dot{a}$) is less power efficient than flying slower (decreasing $|\boldsymbol{V}|$). Long-range migration is an

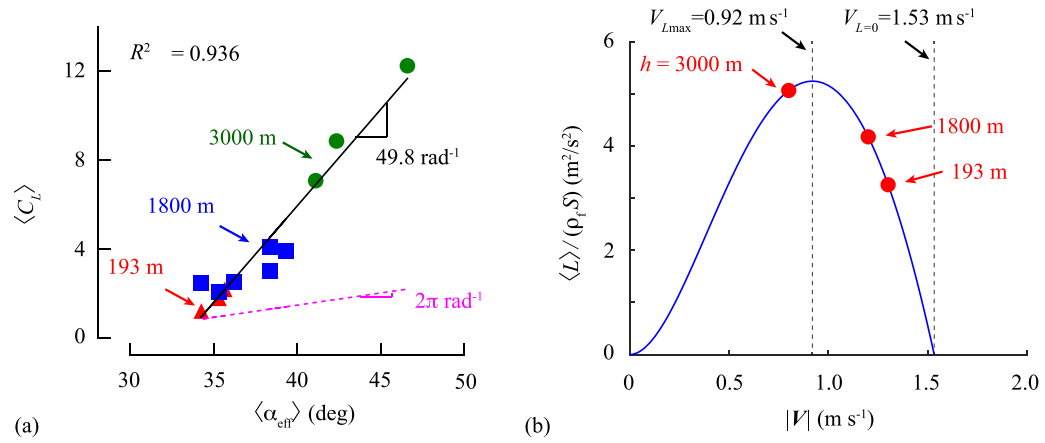

Figure 7. (a) The cycle-averaged lift coefficient $\langle C_L \rangle$ strongly correlates to the cycle-averaged effective angle of attack $\langle \alpha_{eff} \rangle$. (b) Relation between the normalized lift $\langle L \rangle / (\rho_f S)$ and flight speed $|\boldsymbol{V}|$ obtained based on linear regression of $\langle C_L \rangle$ as a function of $\langle \alpha_{eff} \rangle$. Red dots indicate normalized mean lift, calculated with experimentally observed flight speeds at the three altitudes (table 2).

energetically expensive endeavor. Minimizing power during migration is critical in achieving a higher aerodynamic performance.

4. Concluding remarks

The outcomes of this study support the hypothesis that the monarchs are able to produce sufficiently high lift forces to fly in lower density environments. That said, the exact physical mechanism behind the remarkably high lift coefficient produced by the monarchs in thinner air and its impact on the power consumption are currently unknown. One missing variable is the pitching motion of the relatively large, slowly flapping flexible monarch wings. The air density affects the structural dynamic response of the wing deflection, which, in turn, influences the aerodynamic force generation. However modeling the anisotropic monarch wings with complicated vein structure is challenging. Moreover, many butterfly species cannot actively modulate the pitch angle of the wing due to structural constraints [8]. In addition, it is difficult to decipher how much of the pitch motion is active or passive.

Nevertheless, the observations of freely flying monarchs in thinner air and findings from this study contribute to the understanding of the influence of flight attitude in the long-range migration of monarch butterflies from the viewpoint of aerodynamics. Compared to the wealth of research on the aerodynamics of smaller insects (e.g. flies, bees, or dragonflies), or larger flying animals (e.g. birds and bats), the flight of butterflies remains inadequately understood due to their many unique characteristics including the fluid–structure interaction of the wings and wing-body dynamics associated with the body undulation. Further understanding the underlying physical mechanisms behind the long-range insect migration can provide a basis to the creation of bioinspired micro-air vehicles with enhanced flight efficiency and superior flight range.

Acknowledgments

We thank Yusuke Nakamura, Brittany Greene, Munsa Manandhar, M'hamed Ben Moussa and Jack Madden for their help with butterfly measurements and experiments. This work was supported in part by National Science Foundation CBET-1335572 and National Science Foundation CMMI-1761618. Author contributions: conceptualization: CK; Methodology: CK, MKS, DBL, TL; formal analysis: CK, MKS, DBL, HA, SM, TL; investigation: CK, MKS, DBL, HA, TL; software: CK, MKS, SM; visualization: CK, MKS. HA; writing—original draft: CK; writing—review and editing: CK, MKS, DBL, HA, SM, TL; supervision: CK, DBL, HA; Funding acquisition: CK, DBL, TL

ORCID iDs

Madhu K Sridhar https://orcid.org/0000-0001-8801-3057
Chang-Kwon Kang https://orcid.org/0000-0001-9353-4519
Hikaru Aono https://orcid.org/0000-0003-2427-0833
Taeyoung Lee https://orcid.org/0000-0003-4982-4150

References

[1] Dickinson M H, Lehmann F and Sane S P 1999 Wing rotation and the aerodynamics basis of insect flight *Science* **284** 1954–60
[2] Ellington C P, van den Berg C, Willmott A P and Thomas A L R 1996 Leading-edge vortices in insect flight *Nature* **384** 626–30
[3] Shyy W, Aono H, Kang C and Liu H 2013 *An Introduction to Flapping Wing Aerodynamics* (Cambridge: Cambridge University Press)

[4] Srygley R B and Thomas A L R 2002 Unconventional lift-generating mechanisms in free-flying butterflies *Nature* **420** 487–9

[5] Kodali D, Medina C, Kang C and Aono H 2017 Effects of spanwise flexibility on the performance of flapping flyers in forward flight *J. R. Soc. Interface* **14** 20170725

[6] Shyy W, Kang C, Chirarattananon P, Ravi S and Liu H 2016 Aerodynamics , sensing and control of insect-scale flapping-wing flight *Proc. R. Soc.* A **472** 20150712

[7] Fei Y H J and Yang J T 2015 Enhanced thrust and speed revealed in the forward flight of a butterfly with transient body translation *Phys. Rev.* E **92** 033004

[8] Fei Y H J and Yang J T 2016 Importance of body rotation during the flight of a butterfly *Phys. Rev.* E **93** 033124

[9] Suzuki K, Aoki T and Yoshino M 2019 Effect of chordwise wing flexibility on flapping flight of a butterfly model using immersed-boundary lattice Boltzmann simulations *Phys. Rev.* E **100** 013104

[10] Bluman J and Kang C 2017 Wing-wake interaction destabilizes hover equilibrium of a flapping insect-scale wing *Bioinspiration Biomimetics* **12** 046004

[11] Bluman J E, Sridhar M K and Kang C 2018 Chordwise wing flexibility may passively stabilize hovering insects *J. R. Soc. Interface* **15** 20180409

[12] Brower L P, Fink L S and Walford P 2006 Fueling the fall migration of the monarch butterfly *Integr. Comp. Biol.* **46** 1123–42

[13] Brower L P 1996 Monarch butterfly orientation: missing pieces of a magnificent puzzle *J. Exp. Biol.* **199** 93–103

[14] Gibo D L 1981 Altitudes attained by migrating monarch butterflies, Danaus plexippus (Lepidoptera: danainae), as reported by glider pilots *Can. J. Zool.* **59** 571–2

[15] Masters A R, Malcolm S B and Brower L P 1988 Monarch butterfly (Danaus plexippus) thermoregulatory behavior and adaptations for overwintering in Mexico *Ecology* **69** 458–67

[16] Merlin C, Gegear R J and Reppert S M 2009 Antennal circadian clocks coordinate sun compass orientation in migratory monarch butterflies *Science* **325** 1700–4

[17] Zhan S *et al* 2014 The genetics of monarch butterfly migration and warning colouration *Nature* **514** 317–21

[18] Gibo D L and Pallet M J 1979 Soaring flight of monarch butterflies, Danaus plexippus (Lepidoptera: danaidae), during the late summer migration in southern ontario *Can. J. Zool.* **57** 1393–401

[19] Alonso-Mejía A, Rendon-Salinas E, Montesinos-Patiño E and Brower L P 1997 Use of lipid reserves by monarch butterflies overwintering in Mexico: implications for conservation *Ecol. Appl.* **7** 934–47

[20] Slayback D A, Brower L P, Ramirez M I and Fink L S 2007 Establishing the presence and absence of overwintering colonies of the monarch butterfly in Mexico by the use of small aircraft *Am. Entomol.* **53** 28–40

[21] Wassenaar L I and Hobson K A 1998 Natal origins of migratory monarch butterflies at wintering colonies in Mexico: new isotopic evidence *Proc. Natl Acad. Sci. USA* **95** 15436–9

[22] Taylor L R 1974 Insect migration, flight periodicity and the boundary layer *J. Animal Ecol.* **43** 225–38

[23] Betts C R and Wootton R J 1988 Wing shape and flight behaviour in butterflies (Lepidoptera: papilionoidea and hesperioidea): a preliminary analysis *J. Exp. Biol.* **138** 271–88

[24] Le Roy C, Debat V and Llaurens V 2019 Adaptive evolution of butterfly wing shape: from morphology to behaviour *Biol. Rev.* **94** 1261–81

[25] Bomphrey R J, Lawson N J, Harding N J, Taylor G K and Thomas A L R 2005 The aerodynamics of Manduca sexta: digital particle image velocimetry analysis of the leading-edge vortex *J. Exp. Biol.* **208** 1079–94

[26] Fry S N, Sayaman R and Dickinson M H 2005 The aerodynamics of hovering flight in Drosophila *J. Exp. Biol.* **208** 2303–18

[27] Willmott A P and Ellington C P 1997 The mechanics of flight in the hawkmoth Manduca sexta. I. Kinematics of hovering and forward flight *J. Exp. Biol.* **200** 2705–22

[28] Willmott A P, Ellington C P and Thomas A L R 1997 Flow visualization and unsteady aerodynamics in the flight of the hawkmoth, Manduca sexta *Phil. Trans. R. Soc.* B **352** 303–16

[29] Altshuler D L, Dickson W B, Vance J T, Roberts S P and Dickinson M H 2005 Short-amplitude high-frequency wing strokes determine the aerodynamics of honeybee flight *Proc. Natl Acad. Sci. USA* **102** 18213–8

[30] Cheng B, Deng X and Hedrick T L 2011 The mechanics and control of pitching manoeuvres in a freely flying hawkmoth (manduca sexta) *J. Exp. Biol.* **214** 4092–106

[31] Boinski S and Garber P A 2000 *On the Move: How and Why Animals Travel in Groups* (Chicago, IL: University of Chicago Press)

[32] Kang C, Cranford J, Sridhar M K, Kodali D, Landrum D B and Slegers N 2018 Experimental characterization of a butterfly in climbing flight *AIAA J.* **56** 15–24

[33] US Standard Atmosphere 1976 *NASA Technical Report NASA-TM-X-74335* (Washington, DC: NASA)

[34] Lua K B, Lim T T and Yeo K S 2014 Scaling of aerodynamic forces of three-dimensional flapping wings *AIAA J.* **52** 1095–101

[35] Dudley R and Srygley R 1994 Flight physiology of neotropical butterflies: allometry of airspeeds during natural free flight *J. Exp. Biol.* **191** 125–39

[36] Norris A G, Palazotto A N and Cobb R G 2013 Experimental structural dynamic characterization of the hawkmoth (Manduca sexta) forewing *Int. J. Micro Air Vehicles* **5** 39–54

[37] Kang C, Aono H, Cesnik C E S and Shyy W 2011 Effects of flexibility on the aerodynamic performance of flapping wings *J. Fluid Mech.* **689** 32–74

[38] Kang C-K K and Shyy W 2013 Scaling law and enhancement of lift generation of an insect-size hovering flexible wing *J. R. Soc. Interface* **10** 20130361

[39] Henningsson P, Spedding G R and Hedenström A 2008 Vortex wake and flight kinematics of a swift in cruising flight in a wind tunnel *J. Exp. Biol.* **211** 717–30

[40] Wan H, Dong H and Gai K 2014 Computational investigation of cicada aerodynamics in forward flight *J. R. Soc. Interface* **12** 20141116

[41] Liu G, Dong H and Li C 2016 Vortex dynamics and new lift enhancement mechanism of wing–body interaction in insect forward flight *J. Fluid Mech.* **795** 634–51

[42] Li C, Dong H and Zhao K 2018 A balance between aerodynamic and olfactory performance during flight in Drosophila *Nat. Commun.* **9** 3215

[43] Floryan D, Buren T V and Smits A J 2018 Efficient cruising for swimming and flying animals is dictated by fluid drag *Proc. Natl Acad. Sci. USA* **115** 8116–8

[44] Ben-Gida H, Adam K, Taylor Z J, Bezner-Kerr W, Guglielmo C G, Kopp G A and Gurka R 2013 Estimation of unsteady aerodynamics in the wake of a freely flying european starling (Sturnus vulgaris) *PLoS ONE* **8** 0080086

[45] Pennycuick C J 2008 *Modelling the Flying Bird* (Amsterdam: Elsevier)

[46] Graham K, Robert L, Adrian L R, Taylor G K, Nudds R L and Thomas A R L 2003 Flying and swimming animals cruise at a Strouhal number tuned for high power efficiency *Nature* **425** 707–11

[47] Nudds R L, Taylor G K and Thomas A L R 2004 Tuning of Strouhal number for high propulsive efficiency accurately predicts how wingbeat frequency and stroke amplitude relate and scale with size and flight speed in birds *Proc. R. Soc.* B 2071–6

[48] Meng X and Sun M 2016 Wing kinematics, aerodynamic forces and vortex-wake structures in fruit-flies in forward flight *J. Bionic Eng.* **13** 478–90

[49] Dudley R and Ellington C P 1990 Mechanics of forward flight in bumblebees. I. Kinematics and morphology *J. Exp. Biol.* **148** 19–52

[50] Dudley R and Ellington C P 1990 Mechanics of forward flight in bumblebees. II. Quasi-steady lift and power requirements *J. Exp. Biol.* **148** 53–88
[51] Willmott A P and Ellington C P 1997 The mechanics of flight in the hawkmoth manduca sexta. II. Aerodynamic consequences of kinematic and morphological variation *J. Exp. Biol.* **200** 2723–45
[52] Wakeling J M and Ellington C P 1997 Dragonfly flight. III. Lift and power requirement *J. Exp. Biol.* **200** 583–600
[53] Roskam J 2003 *Airplane Design Part I: Preliminary Sizing of Airplanes* (Kansas: DAR Corporation)
[54] Dillon M E and Dudley R 2014 Surpassing Mt. Everest: extreme flight performance of alpine bumble-bees *Biol. Lett.* **10** 20130922
[55] Anderson J D 2017 *Fundamentals of Aerodynamics* 6 edn (New York: McGraw-Hill)
[56] Anderson J M, Streitlien K, Barrett D S and Triantafyllou M S 1998 Oscillating foils of high propulsive efficiency *J. Fluid Mech.* **360** 41–72
[57] Hover F S, Haugsdal Ø and Triantafyllou M S 2004 Effect of angle of attack profiles in flapping foil propulsion *J. Fluids Struct.* **19** 37–47
[58] https://freesvg.org/mountains-in-green
[59] https://snappygoat.com/free-public-domain-images-animal_butterflies_butterfly_insect/35GbXcGgE8enLda5zSbwnA-EL_NgeYmD1gLFGCzsDys.html
[60] https://commons.wikimedia.org/wiki/File:Airplane_Silhouette_R.svg